Chapter

Boundary Element Modeling and Optimization of Three Temperature Nonlinear Fractional Generalized Photo-Thermoelastic Interaction in Anisotropic Semiconductor Structures

Mohamed Abdelsabour Fahmy

Abstract

The main objective of this paper is to introduce a new fractional-order theory called nonlinear fractional generalized photo-thermoelasticity involving three temperatures. Due to strong nonlinearity, it is very difficult to solve the wave problems related to this theory analytically. Therefore, we propose a new boundary element algorithm and technique for simulation and optimization of the considered problems related to this theory. The genetic algorithm (GA) as an optimization method has been applied based on free form deformation (FFD) technique to improve the performance of our proposed technique. In the formulation of the considered problem, the profiles of the considered objects are determined by FFD technique, where the FFD control point positions are treated as genes, and then the chromosome profiles are defined with the gene sequence. The population is established by a number of individuals (chromosomes), where the objective functions of individuals are achieved by the boundary element method (BEM). A nonuniform rational B-spline curve (NURBS) was used to model optimized boundary where it reduces the number of control points and provides the flexibility to design several different shapes for solving the considered photo-thermoelastic wave problems. The numerical results verify the validity and accuracy of our proposed boundary element technique.

Keywords: boundary element method, fractional-order, nonlinear generalized photo-thermoelasticity, three temperatures, modeling and optimization, anisotropic semiconductor structures

1. Introduction

In semiconductors, an electronic deformation leads to local strain which produces plasma waves that are similar to thermal waves generated by local periodic elastic deformation. In general, the electric resistance of semiconductor decreases

with increasing temperature, due to semiconductor electrons released from atoms by heat. Recently, the fractional differential equations that can be used for describing many real-world systems have gotten more and more researchers' attention due to their many applications in sciences and engineering fields.

Recently, increasing attention has been directed toward generalized micropolar thermoelastic problems in anisotropic media due to its many applications in aeronautics, astronautics, geophysics, plasma physics, nuclear plants, nuclear reactors, automobile industries, military technologies, robotics, earthquake engineering, soil dynamics, mining engineering, high-energy particle accelerators, and other engineering industries.

The classical thermoelasticity (CTE) theory has been proposed by Duhamel [1] and Neuman [2] and has two physical paradoxes. First, the heat conduction equation of this theory does not include any elastic terms. Second, the heat conduction equation is of a parabolic type, predicting infinite propagation speed of thermal energy. This prediction is a physically unacceptable situation. Biot [3] developed the classical coupled thermoelasticity (CCTE) theory to resolve the first *paradox* of CTE theory. However, both theories share the second *paradox*. So, several generalizations of Fourier's law that predicts finite propagation speed of thermal waves have been successfully developed and implemented. Lord and Shulman (L-S) [4] proposed the extended thermoelasticity (ETE) theory, where the Fourier's heat conduction law is replaced by the so-called Maxwell-Cattaneo law with one relaxation time. Green and Lindsay (G-L) [5] proposed the temperature rate-dependent thermoelasticity (TRDTE) theory including two relaxation times. Green and Naghdi (G-N) [6, 7] have formulated three different theories in the context of linear generalized thermoelasticity; the general *constitutive assumptions* for the heat flux vector in each theory are different. So, they got three models labeled as types I, II, and III. Type I is based on the classical Fourier's law of heat conduction, type II characterizes the thermoelastic behavior without energy dissipation (TEWOED), and type III describes the thermoelastic interaction with energy dissipation (TEWED). Due to the mathematical difficulties, inherent in solving coupled magnetomechanical problems [8, 9], the problems become too complicated to obtain an analytical solution in a general case. Instead of analytical methods, several numerical methods have recently been successfully developed and implemented to obtain the approximate solutions for such problems including the finite difference method (FDM) [10] and finite element method (FEM) [11]. Nowadays, the boundary element method (BEM) is an effective computational technique [12–31] which provides an excellent alternative to the prevailing finite difference and finite element methods for solving various engineering, scientific, and mathematical applications due to its simplicity, efficiency, and ease of implementation. Throughout the present paper, the new term three-temperature is presented for the first time in the field of photo-thermoelasticity.

The main aim of this paper is to introduce a new fractional-order theory called nonlinear generalized photo-thermoelasticity involving three temperatures. The governing equations of transient thermal stress wave propagation problems associated with this theory are very difficult to solve analytically because of strong nonlinearity. So, we need to develop new numerical techniques for solving such equations. Therefore, we propose a new boundary element technique for solving the governing equations of the proposed theory. The numerical results are depicted graphically to confirm the validity and accuracy of our proposed technique.

A brief summary of this chapter is as follows. Section 1 outlines the background and provides the readers with the necessary information from books and articles for a better understanding of the generalized thermoelastic theories associated with the

distributions of three temperature and thermal stress fields. Section 2 describes the formulation of the new theory and its related problems. Section 3 discusses the implementation of the new BEM to obtain the carrier density field. Section 4 studies the implementation of the new BEM for solving the nonlinear radiative heat conduction equation, to obtain the three temperature fields. Section 5 studies the development of the new BEM and its implementation for solving the move equation based on the known three temperature fields, to obtain the displacement field. Section 6 discusses the shape optimization scheme for semiconductor structures. Section 7 presents the new numerical results that describe the BEM results which are in excellent agreement with the FDM and FEM results.

2. Formulation of the problem

We considered the Cartesian coordinates for a semiconductor structure which occupies the region R and bounded by a closed surface S.

The coupled plasma and thermoelastic wave equations during photothermal process can be written as follows:

The wave equation:

$$\sigma_{ij,j} + \rho F_i = \rho \ddot{u}_i \tag{1}$$

The plasma wave equation:

$$\frac{\partial N}{\partial \tau} - D_0 \nabla^2 N + \frac{1}{\tau_0}(N - n_0) = \check{\alpha}\theta \tag{2}$$

where D_0, N, n_0, τ_0, and $\check{\alpha}$ are the diffusion coefficient, carrier density, equilibrium carrier concentration at temperature θ, electron relaxation time, and thermal expansion coefficient, respectively. Also, we assumed that $\check{\alpha} = \tilde{A}e^{-ax}$.

The two-dimensional three-temperature (2D-3T) radiative heat conduction equations can be expressed as follows:

$$D_\tau^a T_\alpha(r,\tau) = \xi \nabla[\mathbb{K}_\alpha \nabla T_\alpha(r,\tau)] + \xi \overline{\mathbb{W}}(r,\tau), \xi = \frac{1}{c_\alpha \rho \delta_1} \tag{3}$$

where

$$\sigma_{ij} = C_{ijkl}\delta_{ij} - \beta_{ij}\left(\theta + \frac{d_n N}{\check{\alpha}}\right), C_{ijkl} = C_{klij} = C_{jikl}, \beta_{ij} = \beta_{ji} \tag{4}$$

$$\overline{\mathbb{W}}(r,\tau) = \begin{cases} \rho\, \mathbb{W}_{ei}(T_e - T_i) + \rho\, \mathbb{W}_{er}\left(T_e - T_p\right) + \overline{\overline{\mathbb{W}}}, \alpha = e, \delta_1 = 1 \\ -\rho\, \mathbb{W}_{ei}(T_e - T_i) + \overline{\overline{\mathbb{W}}},\ \alpha = i, \delta_1 = 1 \\ -\rho\, \mathbb{W}_{er}\left(T_e - T_p\right) + \overline{\overline{\mathbb{W}}},\ \alpha = p, \delta_1 = \dfrac{4}{\rho} T_p^3 \end{cases} \tag{5}$$

$$\begin{aligned} \overline{\overline{\mathbb{W}}}(r,\tau) = &-\delta_{2n}\mathbb{K}_\alpha \dot{T}_{\alpha,ij} + \beta_{ij} T_{\alpha 0}\left[\text{Å}\delta_{1n}\dot{u}_{i,j} + (\tau_0 + \delta_{2n})\ddot{u}_{i,j}\right] \\ &+ \rho c_\alpha\left[(\tau_0 + \delta_{1n}\tau_2 + \delta_{2n})\ddot{T}_\alpha\right] - \frac{E_g}{\tau_0}(N - n_0) \end{aligned} \tag{6}$$

where

$$\mathbb{W}_{ei} = \rho\mathbb{A}_{ei}T_e^{-2/3}, \mathbb{W}_{er} = \rho\mathbb{A}_{er}T_e^{-1/2}, \mathbb{K}_\alpha = \mathbb{A}_\alpha T_\alpha^{5/2}, \alpha = e, i, \mathbb{K}_p = \mathbb{A}_p T_p^{3+\mathbb{B}} \tag{7}$$

The total energy of unit mass can be described by

$$P = P_e + P_i + P_p, P_e = c_e T_e, P_i = c_i T_i, P_p = \frac{1}{\rho} c_p T_p^4 \tag{8}$$

where σ_{ij} is mechanical stress tensor; ρ is the density; F_i is the mass force vector; u_i is the displacement vector; C_{ijkl} is the constant elastic moduli; β_{ij} are the stress-temperature coefficients; c_e, c_i, and c_p are specific heat capacities of electron, ion, and phonon, respectively; $\mathbb{K}_e, \mathbb{K}_i$, and $\mathbb{K}_p$ are conductive coefficients of electron, ion, and phonon, respectively; $\mathbb{W}_{ei}$ is the electron-ion coefficient; $\mathbb{W}_{ep}$ is the electron-phonon coefficient; the total temperature $\theta = T_e + T_i + T_p$, $-\frac{E_g}{\tau_0}(N - n_0)$ is the recombination term; and E_g is the semiconductor gap energy.

3. BEM solution of carrier density field

In order to construct the integral equation, we use the following Green's function:

$$G(x, \tau) = \frac{e^{-\frac{\tau}{\tau_0}}}{2\sqrt{(\pi D_0 \tau)}} e^{-x^2/4D_0\tau}. \tag{9}$$

We assume that the solution of Eq. (2) can be written as

$$N = n_0 + N'(x, \tau) + \int g(\tau')G(x, \tau - \tau')d\tau', \tag{10}$$

where $G(x, \tau - \tau')$ is a particular solution of Eq. (2) when its right-hand side is equal to zero and $N'(x, \tau)$ is also a particular solution of Eq. (2) which can be obtained as

$$N'(x, \tau) = A\int_0^\tau d\tau' \int_{-\infty}^{\infty} e^{-ax} G(x - x', \tau - \tau')dx'. \tag{11}$$

which can be written in the following form [32].

$$N'(x, \tau) = Ae^{-ax} \frac{\tau_0}{1 - a^2 L_0^2} \left[1 - e^{-\left(1 - a^2 L_0^2\right)\tau/\tau_0}\right], \tag{12}$$

where the minority carrier diffusion length is $L_0 = \sqrt{D_0\tau_0}$. Thus after imposing initial conditions ($N(x, 0) = N_0$ for all x) and boundary conditions ($N(0, \tau) = N_0$ for all τ), we have

$$\int_0^\tau g(\tau')G(0, \tau - \tau')d\tau' = -N'(0, \tau) \tag{13}$$

By solving Eq. (13), the unknown $g(\tau)$ is determined. Then from Eq. (10), we obtain $N(x, \tau)$.

4. BEM solution of temperature field

By applying the Caputo scheme, we have [33].

$$D_{\tau}^{a}T_{\alpha}^{f+1}+D_{\tau}^{a}T_{\alpha}^{f}\approx\sum_{j=0}^{k}W_{a,j}\left(T_{\alpha}^{f+1-j}(r)-T_{\alpha}^{f-j}(r)\right),(\mathrm{f}=1,2,\ldots.,\mathrm{F}),\tag{14}$$

where

$$W_{a,0}=\frac{(\Delta\tau)^{-a}}{\Gamma(2-a)},W_{a,j}=W_{a,0}\Big(\left(j+1\right)^{1-a}-\left(j-1\right)^{1-a}\Big),j=1,2,\ldots.,F.$$

Substituting Eq. (11) into Eq. (3), we obtain

$$\begin{aligned}&W_{a,0}T_{\alpha}^{f+1}(r)-\mathbb{K}_{\alpha}(x)T_{\alpha,II}^{f+1}(r)-\mathbb{K}_{\alpha,I}(x)T_{\alpha,I}^{f+1}(r)\\&=W_{a,0}T_{\alpha}^{f}(r)-\mathbb{K}_{\alpha}(x)T_{\alpha,II}^{f}(r)-\mathbb{K}_{\alpha,I}(x)T_{\alpha,J}^{f}(r)\end{aligned}$$

$$-\sum_{j=1}^{f}W_{a,j}\left(T_{\alpha}^{f+1-j}(r)-T_{\alpha}^{f-j}(r)\right)+\overline{\mathbb{W}}_{m}^{f+1}(x,\tau)+\overline{\mathbb{W}}_{m}^{f}(x,\tau),f=0,1,2,\ldots,F.\tag{15}$$

Based on the fundamental solution which satisfies Eq. (15), the boundary integral equations corresponding to Eq. (3) can be expressed as

$$CT_{\alpha}=\int_{S}\left[T_{\alpha}q^{*}-T_{\alpha}^{*}q\right]dS-\int_{R}\frac{\mathbb{K}_{\alpha}}{D}\frac{\partial T_{\alpha}^{*}}{\partial\tau}T_{\alpha}\,dR.\tag{16}$$

Based on [34], we can write

$$C\,\dot{T}_{\alpha}+H\,T_{\alpha}=G\,Q\tag{17}$$

To solve Eq. (17), the functions T_{α} and q can be interpolated as

$$T_{\alpha}=(1-\theta)T_{\alpha}^{m}+\theta\,T_{\alpha}^{m+1},\tag{18}$$

$$q=(1-\theta)q^{m}+\theta\,q^{m+1}.\tag{19}$$

Differentiating Eq. (18) with time, we obtain

$$\dot{T}_{\alpha}=\frac{dT_{\alpha}}{d\theta}\frac{d\theta}{d\tau}=\frac{T_{\alpha}^{m+1}-T_{\alpha}^{m}}{\tau^{m+1}-\tau^{m}}=\frac{T_{\alpha}^{m+1}-T_{\alpha}^{m}}{\Delta\tau^{m}},\theta=\frac{\tau-\tau^{m}}{\tau^{m+1}-\tau^{m}},0\leq\theta\leq1.\tag{20}$$

By substituting Eqs. (18)-(20) into Eq. (17), we get

$$\left(\frac{C}{\Delta\tau^{m}}+\theta H\right)T_{\alpha}^{m+1}-\theta GQ^{m+1}=\left(\frac{C}{\Delta\tau^{m}}-(1-\theta)H\right)T_{\alpha}^{m}+(1-\theta)GQ^{m}.\tag{21}$$

Thus, the temperature can be determined from the following system:

$$\mathbb{a}\mathrm{X}=\mathbb{b},\tag{22}$$

where $\mathbb{a}$ is an unknown matrix and X and $\mathbb{b}$ are known matrices.

5. BEM solution of displacement field

On the basis of the weighted residual method, the differential equations (1) can be transformed to the following integral equations:

$$\int_R \left(\sigma_{ij,j} + U_i\right) u_i^* \, dR = 0, i,j = 1,2, \ldots ., N \tag{23}$$

in which

$$U_i = \rho F_i - \rho \ddot{u}_i. \tag{24}$$

According to Huang and Liang [35], Eringen [36], and Dragos [37], we can write Eq. (23) as

$$C^n \mathfrak{q}^n = \sum_{j=1}^{N_e} \left[-\int_{\Gamma_j} \mathfrak{p}^* \psi \, d\Gamma \right] \mathfrak{q}^j + \sum_{j=1}^{N_e} \left[\int_{\Gamma_j} \mathfrak{q}^* \psi \, d\Gamma \right] \mathfrak{p}^j, \mathfrak{q} = \psi \, \mathfrak{q}^j, \mathfrak{p} = \psi \, \mathfrak{p}^j \tag{25}$$

which can be written as

$$C^i \mathfrak{q}^i = -\sum_{j=1}^{N_e} \hat{\mathcal{H}}^{ij} \mathfrak{q}^j + \sum_{j=1}^{N_e} \hat{\mathbb{G}}^{ij} \mathfrak{p}^j. \tag{26}$$

This matrix system can be written as follows:

$$\mathbb{H}\mathbb{Q} = \mathbb{G}\mathbb{P}, \tag{27}$$

where $\mathbb{Q}$ represents the displacements and $\mathbb{P}$ represents the tractions.
By using the boundary conditions in Eq. (27), we get

$$\mathbb{A}\,\mathbb{X} = \mathbb{B}, \tag{28}$$

where $\mathbb{A}$ is an unknown matrix and $\mathbb{X}$ and $\mathbb{B}$ are known matrices. We refer the interested readers to Reference [37] for further details.

6. Shape optimization scheme for semiconductor structures

Two criteria can be implemented during shape optimization of semiconductor structures:

I. The minimum global compliance based on the tractions λ and boundary displacements u

$$\mathcal{F} = \frac{1}{2} \int_S (\lambda \bullet u) \, dS, \tag{29}$$

II. The minimum boundary based on the equivalent stresses σ_{ij} and the reference stress σ_0

$$\mathcal{F} = \int_S \left(\frac{\sigma_{ij}}{\sigma_0} \right)^n dS, \tag{30}$$

where n is a natural number.

Based on the boundary displacement u and the reference displacement u_0, we can write

$$\mathcal{F} = \int_S \left(\frac{u}{u_0}\right)^n dS, \tag{31}$$

which can be used to obtain

$$\mathcal{F} = \delta \sum_{k=1}^{M} \left(u^k - \hat{u}^k\right) + \eta \sum_{l=1}^{N} \left(\theta^l - \hat{\theta}^l\right). \tag{32}$$

The efficiency of the proposed technique has been improved using FFD, GA, and the following nonuniform rational B-spline curve (NURBS):

$$C(t) = \frac{\sum_{i=0}^{n} N_{i,o}(t)\varpi_i P_i}{\sum_{i=0}^{n} N_{i,o}(t)\varpi_i}, \tag{33}$$

where $N_{i,o}(t)$ are the B-spline basis functions of order o and ϖ_i are the weights of control points P_i.

7. Numerical results and discussion

The efficiency of our numerical modeling technique has been improved using a nonuniform rational B-spline curve (NURBS) to decrease the computation time and the model's optimized boundary where it reduces the number of control points and provides the flexibility to design a large variety of shapes.

Figure 1 shows the main steps of the genetic algorithm of photo-thermoelastic semiconductor structures.

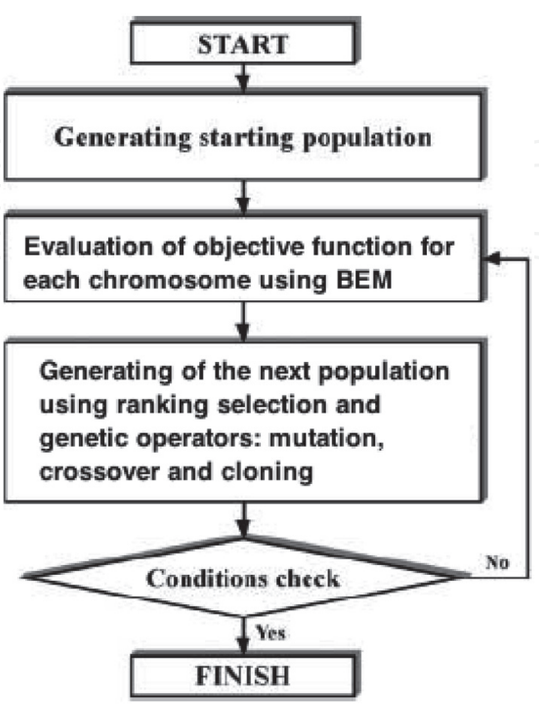

Figure 1.
Genetic algorithm of photo-thermoelastic semiconductor structures.

The design vector is represented by a chromosome x which consists of genes x_i, i = 1, ... , N:

$$x = [x_1, \ldots, x_i, \ldots, x_N] \tag{34}$$

Thus, genes can be considered as design variables.

The following constraints are also imposed on each gene:

$$x_{iL} \leq x_i \leq x_{iR}, i = 1, \ldots, N \tag{35}$$

where x_{iL} and x_{iR} are the left and right admissible values of x_i.

The uniform mutation and boundary mutation are implemented, where the uniform mutation operator replaces a gene of the chromosome with the new random value x_i which corresponds to the design parameter as shown in **Figure 2**.

The uniform mutation probability determines the gene number which will be modified in each population. The boundary mutation operator is a special case of the uniform mutation. The gene after mutation receives one of the boundary values x_{iL} or x_{iR} as shown in **Figure 3**.

The boundary mutation is very useful for boundary element problems in which the solution is on the boundary. The boundary mutation probability determines the gene number which will be modified in each population.

The simple crossover and arithmetical crossover are implemented, where the operator of the simple crossover creates two new chromosomes x′ and y′ from two existing chromosomes selected randomly, x and y, where both chromosomes are coupled together as shown in **Figure 4**.

The simple crossover probability determines the chromosomes number which will be crossing in each population.

The arithmetic crossover operator creates two identical new chromosomes x′ from two existing chromosomes selected randomly, x and y, where the gene values in the new chromosomes are the arithmetic average of genes of the parents as shown in **Figure 5**.

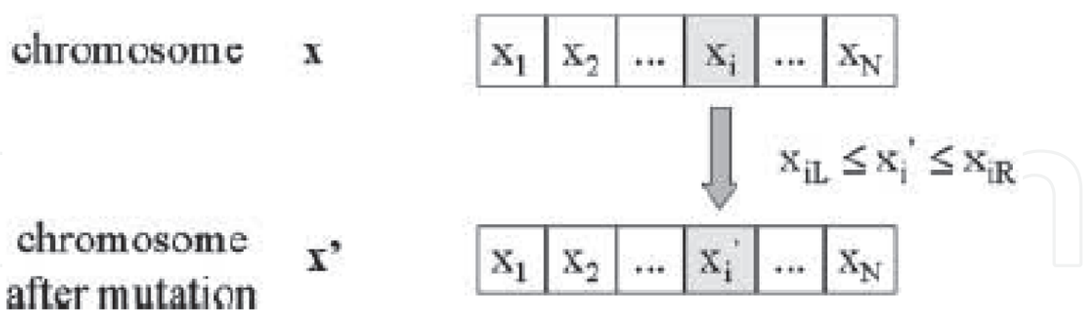

Figure 2.
Implementation of uniform mutation.

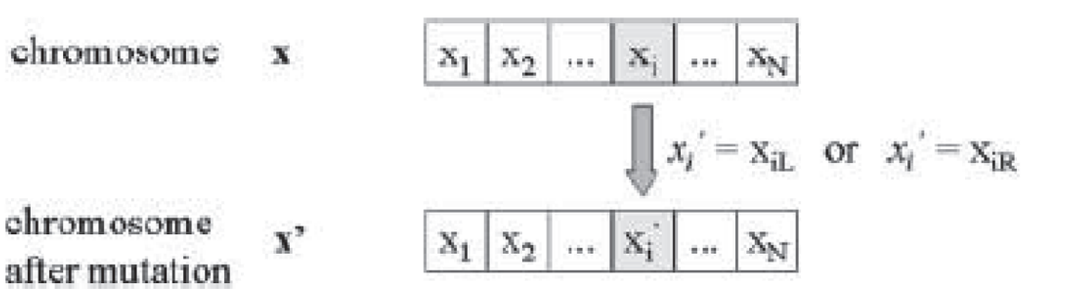

Figure 3.
Implementation of boundary mutation.

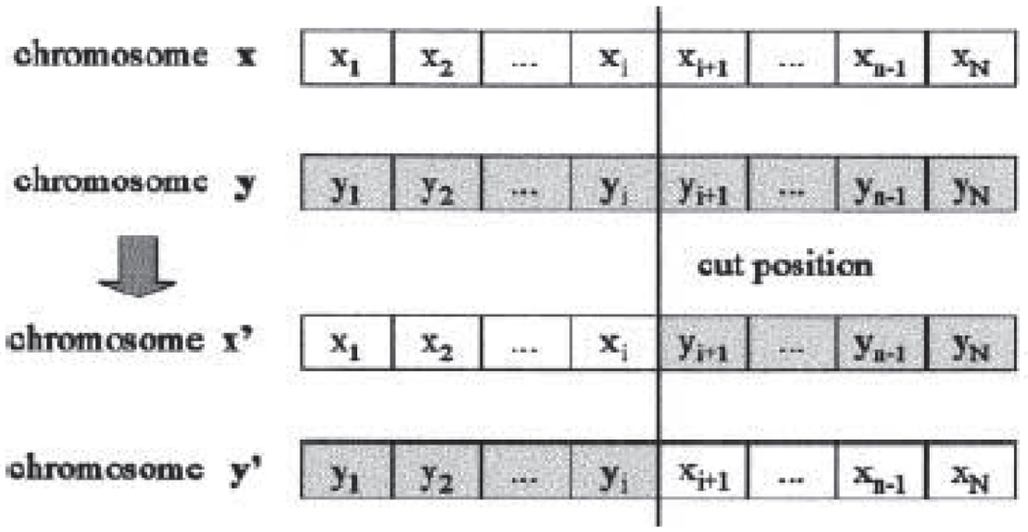

Figure 4.
Implementation of simple crossover.

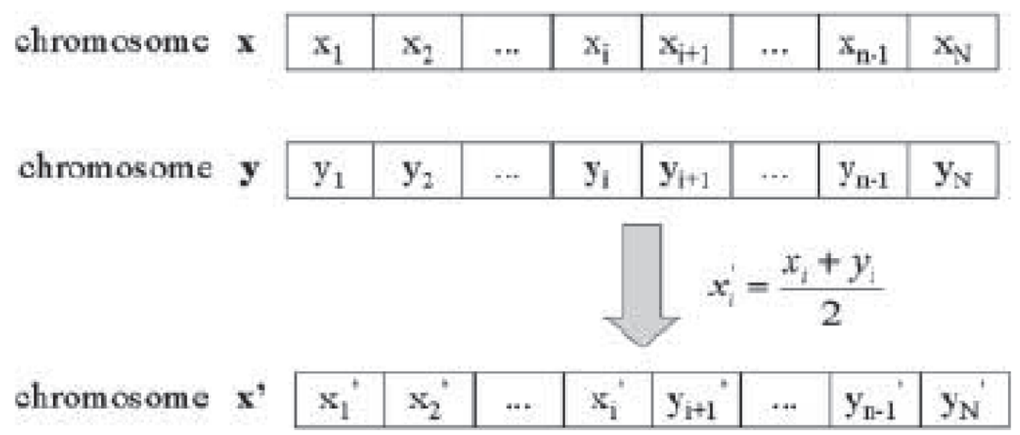

Figure 5.
Implementation of arithmetic crossover.

The operator of the cloning increases the probability of survival of the best chromosome by duplicating this one to the next generation. The probability of the cloning decides how many copies of the best chromosome will be in the new generation.

The ranking selection allows chromosomes to survive with a great value of an objective function. The first step of the ranking selection is sorting all the chromosomes according to the value of the objective function. Then on the basis of the position in the population, the probability of survival is attributed to every chromosome by the following formula:

$$\text{prob}\,(\text{rank}) = q(1-q)^{\text{rank}-1} \tag{36}$$

where rank is the chromosome position after sorting, prob (rank) is the probability of survival, and q is a selection coefficient.

A shape optimization of the photo-thermoelastic semiconductor structure presented in **Figure 6** is considered. Only the parts of the boundary, where the temperature field T_0 and the heat flux q_0 are prescribed, undergo the shape modification.

The optimal shape of the photo-thermoelastic semiconductor structure for isotropic, transversely isotropic, orthotropic, and anisotropic is presented in **Figure 7**. **Table 1** contains the genetic algorithm parameters which were applied.

The efficiency of our numerical modeling technique has been improved using GA, FFD, and NURBS to decrease the computation time of solving three-temperature photo-thermoelastic problems in semiconductor structures. Due to strong nonlinearity, it is very difficult to solve the problems related to this theory analytically. Therefore, we propose a new boundary element model for our current complex problem. So, the validity and accuracy of the proposed technique were confirmed by comparing graphically the one-dimensional results obtained from BEM with those obtained using the finite difference method (FDM) of Pazera and

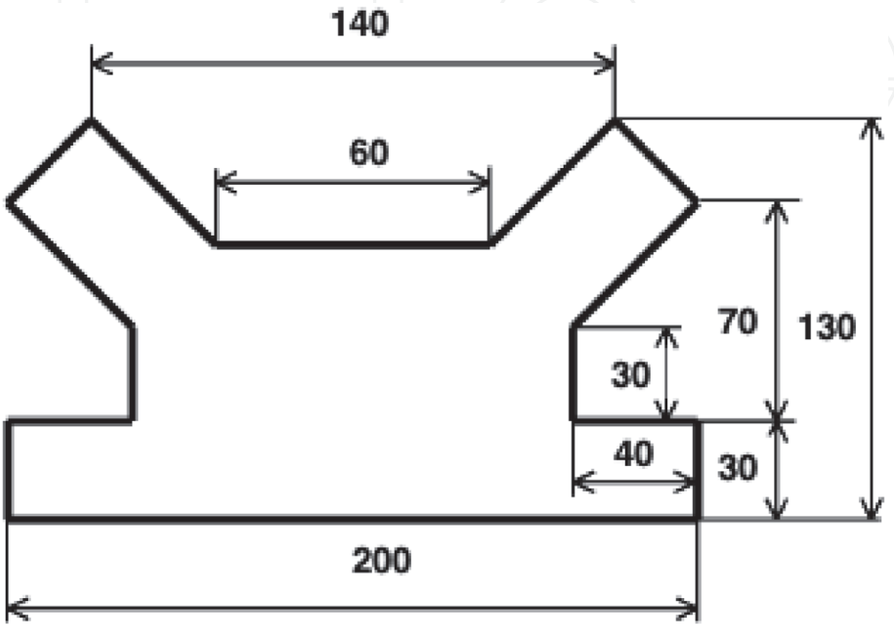

Figure 6.
Optimized considered photo-thermoelastic semiconductor structure.

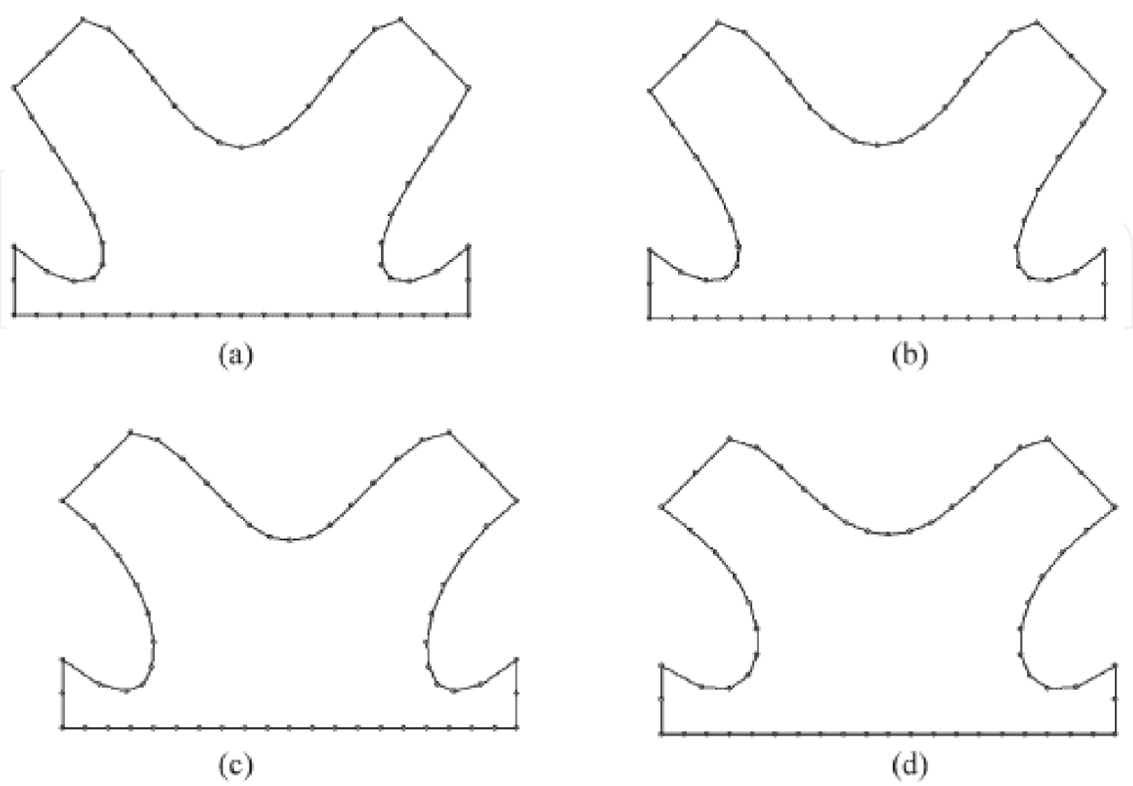

Figure 7.
Optimal shape of photo-thermoelastic semiconductor structure. (a) Isotropic, (b) transversely isotropic, (c) orthotropic, and (d) anisotropic.

Chromosome number	100
Iteration number	150
Design parameter number	5
Uniform mutation probability	0.015
Boundary mutation probability	0.0075
Simple crossover probability	0.075
Arithmetic crossover probability	0.075
Cloning probability	0.05
Selection coefficient	0.1

Table 1.
Parameters of genetic algorithm.

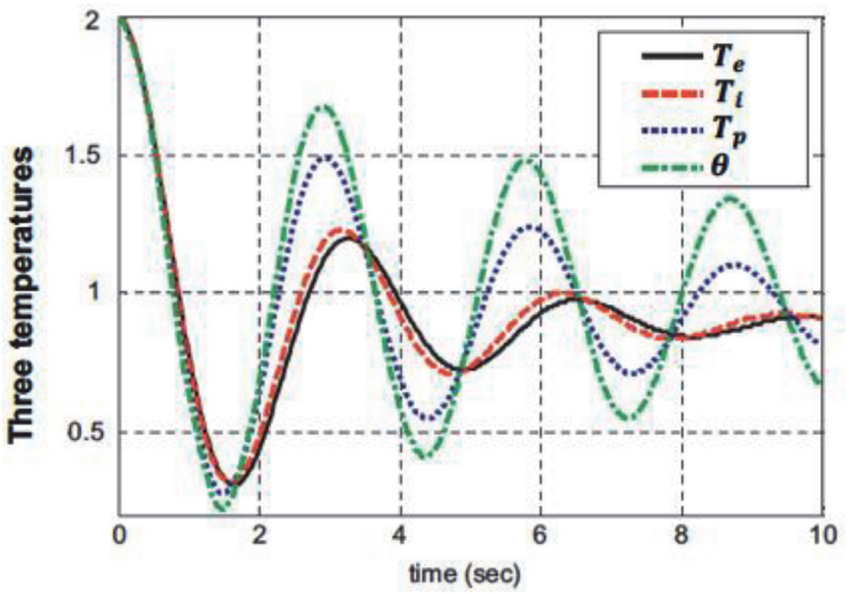

Figure 8.
Variation of the three temperatures $T_e, T_i,$ and T_p with time τ.

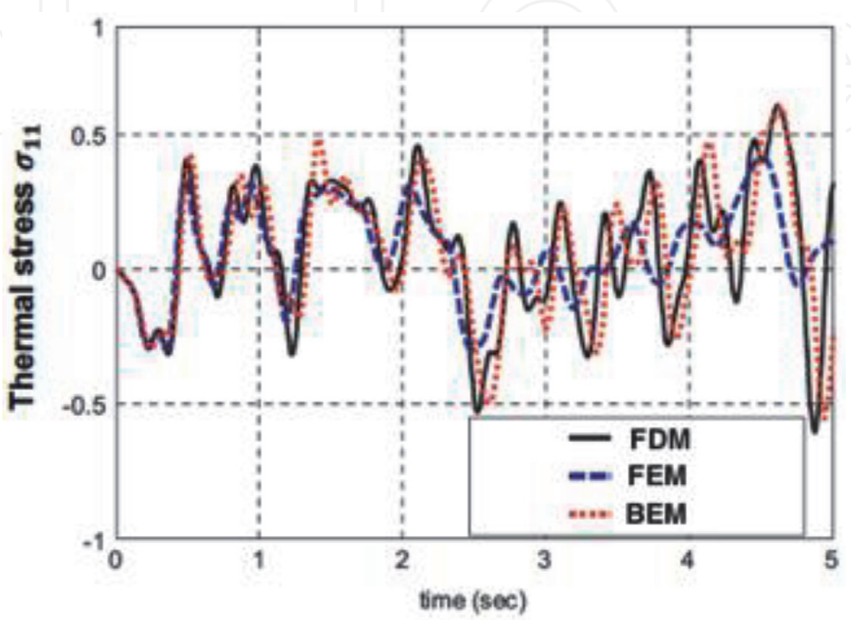

Figure 9.
Variation of the thermal stress σ_{11} with time τ.

Jędrysiak [38] and finite element method (FEM) of Xiong and Tian [39] which have been reduced as a special case from the current problem. For comparison reasons, the 2D-3T radiative heat conduction is replaced by heat conduction. **Figure 8** shows the variations of the temperature T_e, T_i, T_p and $\theta = T_e + T_i + T_p$ with the time τ. The differences between time distributions of electron temperature T_e, ion temperature T_i, phonon temperature T_p, and total temperature θ can be seen from this figure. **Figures 9–11** show the variations of the thermal stresses σ_{11}, σ_{12}, and σ_{22} with the time τ. It can be seen from these figures that the BEM results are in excellent agreement with the FDM and FEM results.

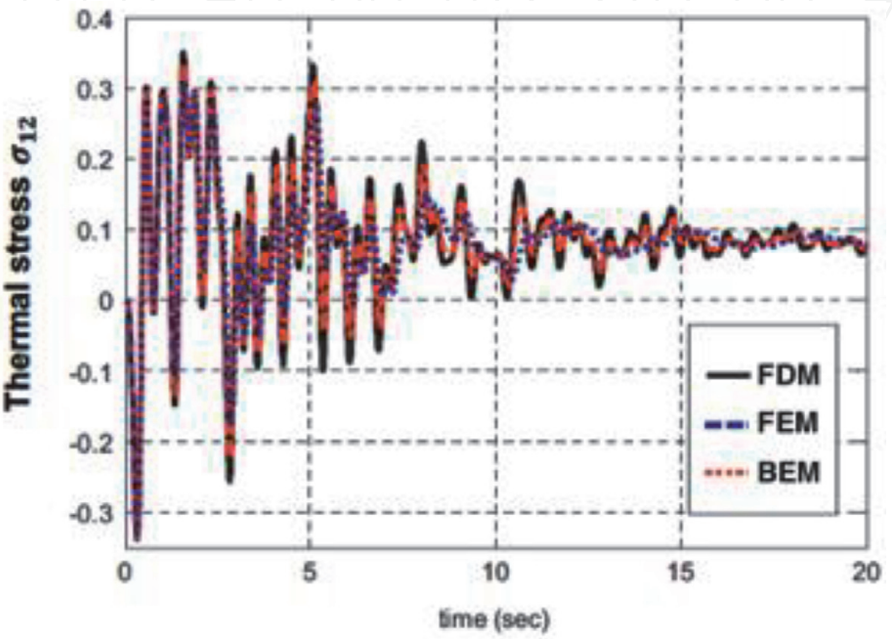

Figure 10.
Variation of the thermal stress σ_{12} with time τ.

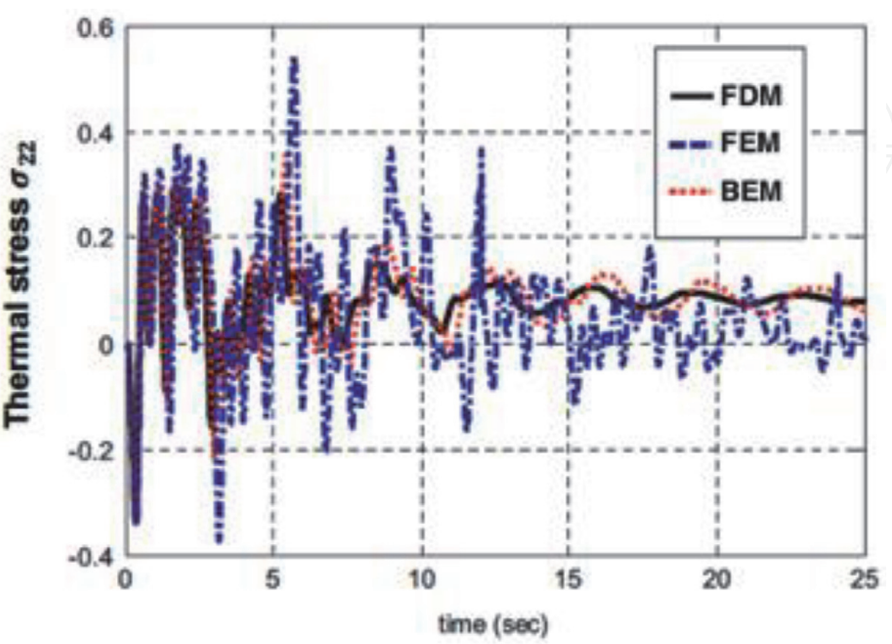

Figure 11.
Variation of the thermal stress σ_{22} with time τ.

8. Conclusion

The aim of this study is to propose a new theory called nonlinear fractional generalized photo-thermoelasticity involving three temperatures and implement a new boundary element technique for modeling and optimization of the three-temperature nonlinear fractional generalized photo-thermoelastic interaction problems in anisotropic semiconductor structures associated with the proposed theory. This technique is implemented based on genetic algorithm (GA), free-form deformation (FFD) method, and nonuniform rational B-spline curve (NURBS) as the global optimization techniques for solving complex problems associated with the proposed theory. FFD is an efficient and accurate technique for treating optimization problems with complex shapes. In the formulation of the considered problem, solutions are obtained for specific arbitrary parameters which are the control point positions in the considered problem; the profiles of the considered objects are determined by FFD method, where the FFD control points positions are treated as genes; and then the chromosomes profiles are defined with the gene sequence. The population is founded by a number of individuals (chromosomes), where the objective functions of individuals are determined by the BEM. The optimal shape of the photo-thermoelastic semiconductor structure for isotropic, transversely isotropic, orthotropic, and anisotropic is obtained. The proposed technique can be applied to a wide range of modeling and optimization problems related with our proposed theory. The numerical results verify the validity and accuracy of our proposed boundary element technique. Also, the BEM is more powerful and simple to use than the FDM or FEM, because it reduces the computational cost. The present numerical results for our general and complex problem may provide interesting information for mechanical engineers, material science researchers, computer scientists, and designers of semiconductor devices.

Author details

Mohamed Abdelsabour Fahmy
Faculty of Computers and Informatics, Suez Canal University, Ismailia, Egypt

*Address all correspondence to: mohamed_fahmy@ci.suez.edu.eg

References

[1] Duhamel J. Some memoire sur les phenomenes thermo-mechanique. Journal de l'École polytechnique. 1837;**15**:1-57

[2] Neumann F. Vorlesungen Uber die theorie der elasticitat. Brestau: Meyer; 1885

[3] Biot M. Thermoelasticity and irreversible thermo-dynamics. Journal of Applied Physics. 1956;**27**:249-253

[4] Lord HW, Shulman Y. A generalized dynamical theory of thermoelasticity. Journal of the Mechanics and Physics of Solids. 1967;**15**:299-309

[5] Green AE, Lindsay KA. Thermoelasticity. Journal of Elasticity. 1972;**2**:1-7

[6] Green AE, Naghdi PM. On undamped heat waves in an elastic solid. Journal of Thermal Stresses. 1992;**15**:253-264

[7] Green AE, Naghdi PM. Thermoelasticity without energy dissipation. Journal of Elasticity. 1993; **31**:189-208

[8] Kaliski S. Thermo-magneto-microelasticity. Bulletin of the Polish Academy of Sciences: Technical Sciences. 1968;**16**:7-12

[9] Jafarian A, Ghaderi P, Golmankhaneh AK, Baleanu D. Analytic solution for a nonlinear problem of magneto-thermoelasticity. Reports on Mathematical Physics. 2013;**71**:399-411

[10] Abd-Alla AM, El-Naggar AM, Fahmy MA. Magneto-thermoelastic problem in non-homogeneous isotropic cylinder. Heat and Mass Transfer. 2003; **39**:625-629

[11] Abbas IA, Abd-alla AN, Othman MIA. Generalized magneto-thermoelasticity in a fiber-reinforced anisotropic half-space. International Journal of Thermophysics. 2011;**32**: 1071-1085

[12] Fahmy MA. Thermoelastic stresses in a rotating non-homogeneous anisotropic body. Numerical Heat Transfer: Part A Applications. 2008;**53**:1001-1011

[13] Fahmy MA. A time-stepping DRBEM for magneto-thermo-viscoelastic interactions in a rotating nonhomogeneous anisotropic solid. International Journal of Applied Mechanics. 2011;**3**:1-24

[14] Fahmy MA. A time-stepping DRBEM for the transient magneto-thermo-visco-elastic stresses in a rotating non-homogeneous anisotropic solid. Engineering Analysis with Boundary Elements. 2012;**36**:335-345

[15] Fahmy MA. Transient magneto-thermoviscoelastic plane waves in a non-homogeneous anisotropic thick strip subjected to a moving heat source. Applied Mathematical Modelling. 2012; **36**:4565-4578

[16] Fahmy MA. Numerical modeling of transient magneto-thermo-viscoelastic waves in a rotating nonhomogeneous anisotropic solid under initial stress. International Journal of Modeling, Simulation, and Scientific Computing. 2012;**3**:1250002

[17] Fahmy MA. The effect of rotation and inhomogeneity on the transient magneto-thermoviscoelastic stresses in an anisotropic solid. Journal of Applied Mechanics. 2012;**79**:1015

[18] Fahmy MA. Transient magneto-thermo-viscoelastic stresses in a rotating nonhomogeneous anisotropic solid with and without a moving heat source. Journal of Engineering Physics and Thermophysics. 2012;**85**:950-958

[19] Fahmy MA. Transient magneto-thermo-elastic stresses in an anisotropic viscoelastic solid with and without moving heat source. Numerical Heat Transfer: Part A Applications. 2012;**61**:547-564

[20] Fahmy MA. Implicit-explicit time integration DRBEM for generalized magneto-thermoelasticity problems of rotating anisotropic viscoelastic functionally graded solids. Engineering Analysis with Boundary Elements. 2013; **37**:107-115

[21] Fahmy MA. Generalized magneto-thermo-viscoelastic problems of rotating functionally graded anisotropic plates by the dual reciprocity boundary element method. Journal of Thermal Stresses. 2013;**36**:1-20

[22] Fahmy MA. A three-dimensional generalized magneto-thermo-viscoelastic problem of a rotating functionally graded anisotropic solids with and without energy dissipation. Numerical Heat Transfer: Part A Applications. 2013;**63**:713-733

[23] Fahmy MA. A computerized DRBEM model for generalized magneto-thermo-visco-elastic stress waves in functionally graded anisotropic thin film/substrate structures. Latin American Journal of Solids and Structures. 2014;**11**:386-409

[24] Fahmy MA. Computerized Boundary Element Solutions for Thermoelastic Problems: Applications to Functionally Graded Anisotropic Structures. Saarbrücken: LAP Lambert Academic Publishing; 2017

[25] Fahmy MA. Boundary Element Computation of Shape Sensitivity and Optimization: Applications to Functionally Graded Anisotropic Structures. Saarbrücken: LAP Lambert Academic Publishing; 2017

[26] Fahmy MA. Shape design sensitivity and optimization for two-temperature generalized magneto-thermoelastic problems using time-domain DRBEM. Journal of Thermal Stresses. 2018;**41**: 119-138

[27] Fahmy MA. Shape design sensitivity and optimization of anisotropic functionally graded smart structures using bicubic B-splines DRBEM. Engineering Analysis with Boundary Elements. 2018;**87**:27-35

[28] Fahmy MA. Boundary element algorithm for modeling and simulation of dual phase lag bioheat transfer and biomechanics of anisotropic soft tissues. International Journal of Applied Mechanics. 2018;**10**:1850108

[29] Fahmy MA. Modeling and optimization of anisotropic viscoelastic porous structures using CQBEM and moving asymptotes algorithm. Arabian Journal for Science and Engineering. 2019;**44**:1671-1684

[30] Fahmy MA. Boundary element modeling and simulation of biothermomechanical behavior in anisotropic laser-induced tissue hyperthermia. Engineering Analysis with Boundary Elements. 2019;**101**:156-164

[31] Fahmy MA. A new LRBFCM-GBEM modeling algorithm for general solution of time fractional order dual phase lag bioheat transfer problems in functionally graded tissues. Numerical Heat Transfer: Part A Applications. 2019;**75**:616-626

[32] De Mey G. An integral equation method to calculate the transient behavior of a photovoltaic solar cell. Solid-State Electronics. 1978;**21**:595-596

[33] Cattaneo C. Sur une forme de i'equation de la chaleur elinant le paradox d'une propagation instantanc. Comptes Rendus de l'Académie des Sciences. 1958;**247**:431-433

[34] Wrobel LC, Brebbia CA. The dual reciprocity boundary element

formulation for nonlinear diffusion problems. Computer Methods in Applied Mechanics and Engineering. 1987;**65**:147-164

[35] Huang FY, Liang KZ. Boundary element method for micropolar thermoelasticity. Engineering Analysis with Boundary Elements. 1996;**17**:19-26

[36] Eringen AC. Theory of micropolar elasticity. In: Liebowitz H, editor. Fracture. New York: Academic Press; 1968

[37] Dragos L. Fundamental solutions in micropolar elasticity. International Journal of Engineering Science. 1984;**22**: 265-275

[38] Pazera E, Jędrysiak J. Effect of microstructure in thermoelasticity problems of functionally graded laminates. Composite Structures. 2018; **202**:296-303

[39] Xiong QL, Tian XG. Generalized magneto-thermo-microstretch response during thermal shock. Latin American Journal of Solids and Structures. 2015; **12**:2562-2580